Indian J Phys
https://doi.org/10.1007/s12648-021-02242-7

ORIGINAL PAPER

First-principles calculations to investigate variation of cationic-ligand $LmAl_2Ge_2$ (Lm = Ca, Y, La and Ce)

Z Zada[1], A A Khan[2], R Zada[3], A H Reshak[4,5,6]*, G Murtaza[7,8], M Saqib[9], M M Ramli[6] and J Bila[4]

[1]Materials Modelling Lab, Department of Physics, Islamia College University, Peshawar, Pakistan

[2]Department of Physics, University of Peshawar, Peshawar, Pakistan

[3]Institute of Chemical Science, University of Peshawar, KPK, Peshawar, Pakistan

[4]Physics Department, College of Science, University of Basrah, Basrah 61004, Iraq

[5]Department of Instrumentation and Control Engineering, Faculty of Mechanical Engineering, Czech Technical University in Prague, Technicka 4, 166 07, Prague 6, Czech Republic

[6]Center of Excellence Geopolymer and Green Technology (CEGeoGTech), University Malaysia Perlis, 01007 Kangar, Perlis, Malaysia

[7]Materials Modeling Lab, Department of Physics, Islamia College Peshawar, P.O. Box 25120, Peshawar, Pakistan

[8]Department of Mathematics and Natural Sciences, Prince Mohammad Bin Fahd University, P. O. Box 1664, Alkhobar 31952, Kingdom of Saudi Arabia

[9]Department of Electrical and Computer Engineering, COMSATS University Islamabad, Abbottabad Campus, KPK, Islamabad, Pakistan

Received: 06 April 2021 / Accepted: 12 November 2021

Abstract: Detailed cationic-ligand variation for $LmAl_2Ge_2$ (Lm = Ca, Y, La and Ce) compounds has been examined under the framework of full potential augmented plane wave (FP-APW) employed within density functional theory (DFT). Our theoretical computational calculations confirm reliable results, to experimentally mentioned data. We establish that ferromagnetic phase is more stable and also acceptable for magnetic properties. The designed band structures and projected density of state (DOS) of $LmAl_2Ge_2$ confirm metallic character along with strong hybridization of (Ca, Y, La) *d* and Ce *f* states with (Al, Ge) *p* states. Furthermore, the analysis of magnetic properties of $CaAl_2Ge_2$, YAl_2Ge_2 and $LaAl_2Ge_2$ compounds shows weak ferromagnetic character as compared to $CeAl_2Ge_2$ compound.

Keywords: DFT; Rare-earth pnictogens; Band profiles; Ferromagnetic phase; DFT; Spin ordering; Metallic nature; Ferromagnetic character

1. Introduction

Generally, intermetallics phase holds large impact in the broad range series of applications from shape memory alloys, computer read, jewelry and dentistry [1, 2] and is also used for technological outcome as "colossal" or else "giant" magneto-resistive (CMR or else GMR) materials where magneto-resistance within metallic thin films is able to alter resistivity with respect to external magnetic field [3–7]. Although the major application of *GMR* can be basically utilized as spin valves, spin filters and magnetic field sensors [8, 9], the main applications of *GMR* are valuable for magnetic sensors, which are usefully used to read-heads in the hard disk drives, microelectromechanical systems (MEMS), biosensors, and so on.

Broadly intermetallic phases having the formula AM_2X_2 (*A* = rare-earth metals or else alkaline earth, *M* = d-block metals; *X* = Group 13–15 elements) include two omnipresent structure types, $ThCr_2Si_2$ (14/mmm) and $CaAl_2Si_2$ ($P\acute{3}m1$), correspondingly [10]. However, researchers have utilized various crystal structure types to illustrate that the requirement for arrangement of pristine $CaAl_2Si_2$ structure-type consistence along with particular conditions, recognized as the entire numeral of valence electrons mainly present in per formula unit, must be equal to or less than 16

*Corresponding author, E-mail: maalidph@yahoo.co.uk

Published online: 09 February 2022

[11–13]. The previously known pnictide AM_2Y_2 (A: electro-positive element; M: metal; Y: P–Bi) is pursued with no exemption into this scheme, which initially in contradicting associations $L_nLi_2Y_2$ (L_n: Pr, Ce, Tb, Nd; Y: P–Bi) [14–16] correctly changes into correct ($L_nLi_3Y_2$) composition [17]. The merely well-known silicides ($L_nAl_2Si_2$) as well as layered ligand germanides characterized by the chemical formula of ($L_nAl_2Ge_2$) persist [18–21], which primarily crystallize in the pristine crystal structure ($CaAl_2Si_2$), as reported, e.g., $[Ln^{3+}(Al^{3+})_2(Si^{4-})_2]$ has no valance composition. In view of the fact that the structural information of $GdAl_2Si_2$ [21] shows a similar distribution of cation ligands according to the given formula which are same and should be applicable for the case of germanide also, it has a certain outward aspect to benefit from this connection similarly to study their electronic character more strongly.

At the silicides (trivalent rare-earth metals) side, so far just a crystal structure determination of $GdAl_2Si_2$ was presented, while $CeAl_2Si_2$ [22] and YAl_2Si_2 [23] compounds were figure it out and published the lattice constants for the first time. Additionally, no doubt existed in previous works but similar and comparable connections established with (Ln = Gd-Lu, Pr), but no other features of crystallographic and magnetic information were described [18, 19].

The compound $L_nAl_2Si_2$ (L_n: Y, trivalent rare-earth metal) has been synthesized by increasing the temperature from 800° to 1000 °C. They are crystallized in the ($CaAl_2Si_2$) pristine structure ($P\bar{3}m1$; $Z = 1$), and it belongs to isotypic [24]. For the band structure investigation of both $CaAl_2Si_2$ and YAl_2Si_2, LMTO code was designed, the YAl_2Si_2 confirms non-electrovalent makeup with respect to given formula, and this compound is also discussed in that category by means of electrical conductivity and mainly from the bonding mechanism side [24]. From characterization, it clears that motley crystal $GdAl_{2-x}Mn_xSi_2$ varies from $GdAl_2Si_2$ ($CaAl_2Si_2$) to $GdMn_2Si_2$ ($ThCr_2Si_2$) when we utilize value of Mn ($x \approx 0.3$). Further the crystallization of $EuAl_2Ge_2$, $EuAl_2Si_2$ and $YbAl_2Ge_2$ was done by means of heating from 1070 to 1270 K in same structural phase. The compounds $EuAl_2Ge_2$ and $EuAl_2Si_2$ examined paramagnetic character beyond at 50 K. Furthermore, the compounds $EuAl_2Ge_2$ and $EuAl_2Si_2$ show antiferromagnetic ordering at the value of $T_N = 27.5$ K and $T_N = 35.5$ K correspondingly [25].

The usual response of $YbAl_2Si_2$ compound has been identified from 100 to 300 K in the range of temperature. The linear analysis of inverse susceptibility provides us value of temperature with a lesser magnetic moment value of 2.57 μ_B (Yb) along with extremely examined negative paramagnetic (T_c) Curie temperature of near about − 382 K. Below 100 K temperature, the degree level of divalent ytterbium has grown sharply [25]. Furthermore, the non-magnetic $4f^{14}$ suitable ground states were examined in Yb basal compounds; however, near the Fermi level the high, sharp 4*f* shows the capability to generate mediate valency within $YbAl_2Si_2$. Moreover, the details behind their stability are a vanishing band gap when the present atoms in M_2X_2 slabs demonstrate slight electronegativity dissimilarity. Considered for this position, the excessive electrons do not play a role in making the crystal structure unstable, whereas it occurred when the energy gap is present. Consequently, it clears that the metallic response is not due to the existence of the excessive electrons, but actually from metallic character itself [24]. Separately, each compound AAl_2Ge_2 and $CaAl_2Si_2$ crystal structure type is probable shows metallic nature; anyhow the valence shell electron is based for metal A.

The SEM and XRD are used for the characterization of ternary as well as binary silicides, ($DyAl_2Si_2$, $DySi_2$) with Al and Si solid solution correspondingly. Even after annealing, the phase mixture stays unaffected [26]. Both aluminum silicides and aluminum germanides AAl_2X_2 (A = alkaline or else rare-earth metal and X = Ge or else Si) [27, 28] were crystallized in the trigonal [La_2O_3] structure [29], wherever ordered double-puckered hexagonal layers are prearranged chemically of Ge (Si) and Al atoms even as intercalated A (cations) atoms are there. The stability of these major compounds was astonishing due to their negligible difference in electronegativity between the double-layer atoms. Further the electron–phonon interaction and electronic structure have been analyzed for YAl_2Si_2 compound [30]. By first-principles calculations, various other families of compounds like Heusler's [31–34], anti-fluorite [35], zintl phases [36–40], rare-earth (RE) pnictide [51], halides and ternary alloys [52, 53], skutterudites [54] and chalcogenides [55, 56] are studied so far which are well known for their structure, electronic, magnetic and other functional applications.

Researchers have worked to study the physical properties of $LmAl_2Ge_2$ compounds experimentally [20, 24, 28, 50], but still, the lack of theoretical study chiefly on structural, physical, electronic and magnetic properties for understudied compounds was untouched mainly by utilizing DFT. In this work, our concentration is mostly focused on the enhancement of energy band gap to cover-up the deficiency of theoretical information and give complete package concerning with $LmAl_2Ge_2$ compounds by means of FP-APW method. Furthermore, the calculated work is significant not only due to its novelty, but it delivers attractive results of materials which have appropriate properties for their use in coming future advance innovations.

2. Computational calculations in detail

The $LmAl_2Ge_2$ compounds are classified as intermetallic phases and analyzed in trigonal structure with space group (No. 164) [28]. The calculations were accomplished employing density functional theory (DFT) [41, 42] based on FP-APW approach as summarized in WIEN2K code [43]. Further by treating exchange plus correlation potential, we utilized approximation techniques specifically as GGA-PBE [44] and GGA + U [45, 46]. The optimized lattice parameters are determined by using the PBE-GGA functional. The relaxed geometry after that used to examine the band structure, the density of states (total and partial), whole magnetic moments of these compounds. GGA + U is more precise generalized approximation as linked to LDA/PBE-GGA. Though LDA is deficient because it has been used for slowly varying density, it fails when the density rapidly changes. GGA is a useful approximation as compared to LDA because in molecules it contains the gradient of density at their coordinates and it gives better results in domain of the molecular geometrics in the ground state energies, but d states are basically not bound. The generalized gradient approximation (GGA) can be expressed as:

$$E_{xc}^{GGA}(n_\uparrow, n_\downarrow) = \int \epsilon_{xc}(n_\uparrow, n_\downarrow, \nabla n_\uparrow, \nabla n_\downarrow) n(r) d^3 r \qquad (1)$$

Here, $n_\uparrow, n_\downarrow$ represent electron charge densities for spin-up and spin-down channel correspondingly and $\nabla n_\uparrow, \nabla n_\downarrow$, are the corresponding gradients enhancement. More facts about the FM method are proposed in the present calculations. To report self-interaction inaccuracy in *d* states, we proposed the GGA + U method, which provides us high treatment of the electron correlation by means of Hubbard model. The parameter U can be observed through linear response theory [57, 58]. We have used U_{eff} = 7 eV to treat only d and f states. Moreover, spherical harmonics were organized within help of prime functions electron densities as well as potential by circular atomic sites within cutoff value of l_{max} = 10, while the charge density is Fourier expanded up to G_{maxi} = 12 atom unit $(au)^{-1}$, where G_{maxi} is major vector within Fourier expansion. The wave functions are enlarged in extent in interstitial domain (ID) to plane waves within cutoff value of $K \times$ max = 7.0/*R*MT, where average value of radius of muffin–tin spheres provides us *R*MT plus *K*max symbolizes the larger magnitude of K vector in plane wave. We pick value of non-overlapping muffin–tin radii like (2.5, 2.16, 2.39), (2.5, 2.09, 2.31), (2.5, 2.17, 2.4) and (2.5, 2.0, 2.23) au for $CaAl_2Ge_2$, YAl_2Ge_2, $LaAl_2Ge_2$ and $CeAl_2Ge_2$ elements in that order. We utilized 1000 k points Monkhorst–Pack mesh [47, 48] in Brillion zone intended for these compounds in ferromagnetic phase.

3. Results and discussion

3.1. Structural properties

$LmAl_2Ge_2$ has been prearranged in hexagonal structure [Fig. 1(a)] [49], associated with the known flawless $CaAl_2Si_2$ structure. The Al bilayer exists as a corrugated (puckered) Al honeycomb, though these compounds crystallize in the trigonal ($CaAl_2Si_2$) structure. The analysis of ($ThCr_2Si_2$) structure is motivating one on account of many compounds which own this type symmetry and also illustrate supreme properties with respect to $CaAl_2Si_2$ type. Lesser numbers of compounds crystallize on $CaAl_2Si_2$ symmetry, because diverse and obvious features between these two types are electronic flexibility [3–7]. $CaAl_2Si_2$ type is determined merely when the B-site (Al) element has (d^{10}, d^5 or d^0) electronic configurations [11]. The $CaAl_2Si_2$ type is acceptable with respect to $ThCr_2Si_2$ type for d^{10} and d^0 configurations.

The $LmAl_2Ge_2$ (Lm = Y, Ca, Ce, A) compounds exhibit the trigonal crystal geometry. The designed plots of optimization and optimized structural parameters are depicted in Fig. 2 and Table 1. In intended plots of optimization, the optimized volume is termed as ferromagnetic phase.

The structural theoretical parameters are determined by volume optimization process, and these structural parameters consists of lattice constants a (Å) as well as c (Å), B(GPa), bulk modulus and pressure derivative of bulk modulus (Bp). To find out the whole stable energy (E_0), we used the "Birch–Murnaghan's equation of state." The designed optimization plots give lowest suitable energy of the primitive unit cell.

The lattice constants of our mentioned compounds are strictly interrelated through the experimental values [28, 50]. The lattice constants *a* (Å) as well as *c* (Å) of the compounds increase as we change the cation ligands from Ca to Ce. The step-up of lattice constants is due to the large atomic size as well as volume.

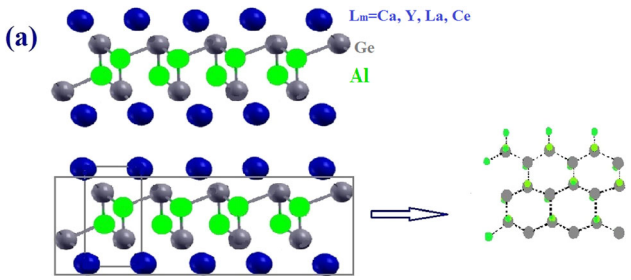

Fig. 1 Crystal configuration of $LmAl_2Ge_2$ (Lm = Ca, Y, La, Ce). Blue spheres: *Lm*; gray spheres: Al; green spheres: Ge. The tetrahedral coordination of Al atoms along with Al_2Ge_2 poly-anion is emphasized

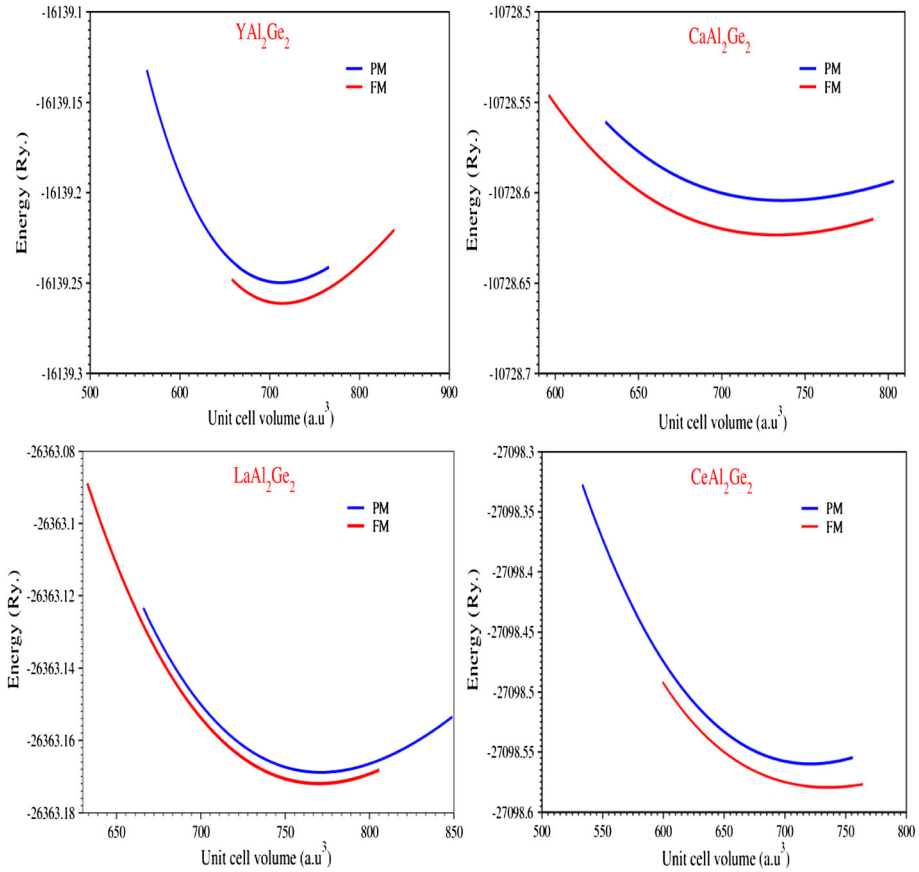

Fig. 2 Optimized plots of total energy as a function of the unit cell volume for $LmAl_2Ge_2$ (Lm = Y, Ca, La, Ce)

Table 1 Optimized structural parameters of $LmAl_2Ge_2$ compounds

Comps	Lattice constant (Å) This work		Exp (Å)		V_0 (a.u)^3	B(GPa)	Bp	E_0 (Ry)	
	a	c	a	c				FM	PM
$CaAl_2Ge_2$	4.120	7.160	4.175[a]	7.173[a]	732.830 108.28[b]	63.381	3.820	− 10,728.603	− 10,728.559
YAl_2Ge_2	4.103	7.040	4.205[a]	6.699[a]	713.950 102.58[c]	74.760	5.000	− 16,139.251	− 16,139.249
$LaAl_2Ge_2$	4.255	7.070	4.297[a]	7.013[a]	769.950 112.14[b]	72.472	3.780	− 26,363.171	− 26,363.170
$CeAl_2Ge_2$	4.330	7.270	4.283[d]	6.925[d]	720.920 110[d]	101.571	2.200	− 27,098.559	− 27,098.558

[a]Ref. [28]
[b]Ref. [24]
[c]Ref. [20]
[d]Ref. [50]

3.2. Electronic properties

The energy band structures of $CaAl_2Ge_2$, YAl_2Ge_2, $LaAl_2Ge_2$ and $CeAl_2Ge_2$ compounds calculated by so-called GGA-PBE and GGA + U approximations along with the Brillouin zone are exposed in Fig. 3, as well as Fig. 4, in that order. The reference point so-called Fermi level is positioned at zero energy. The band structures of considered materials were plotted using symmetry points (Γ-M–K-Γ-A).

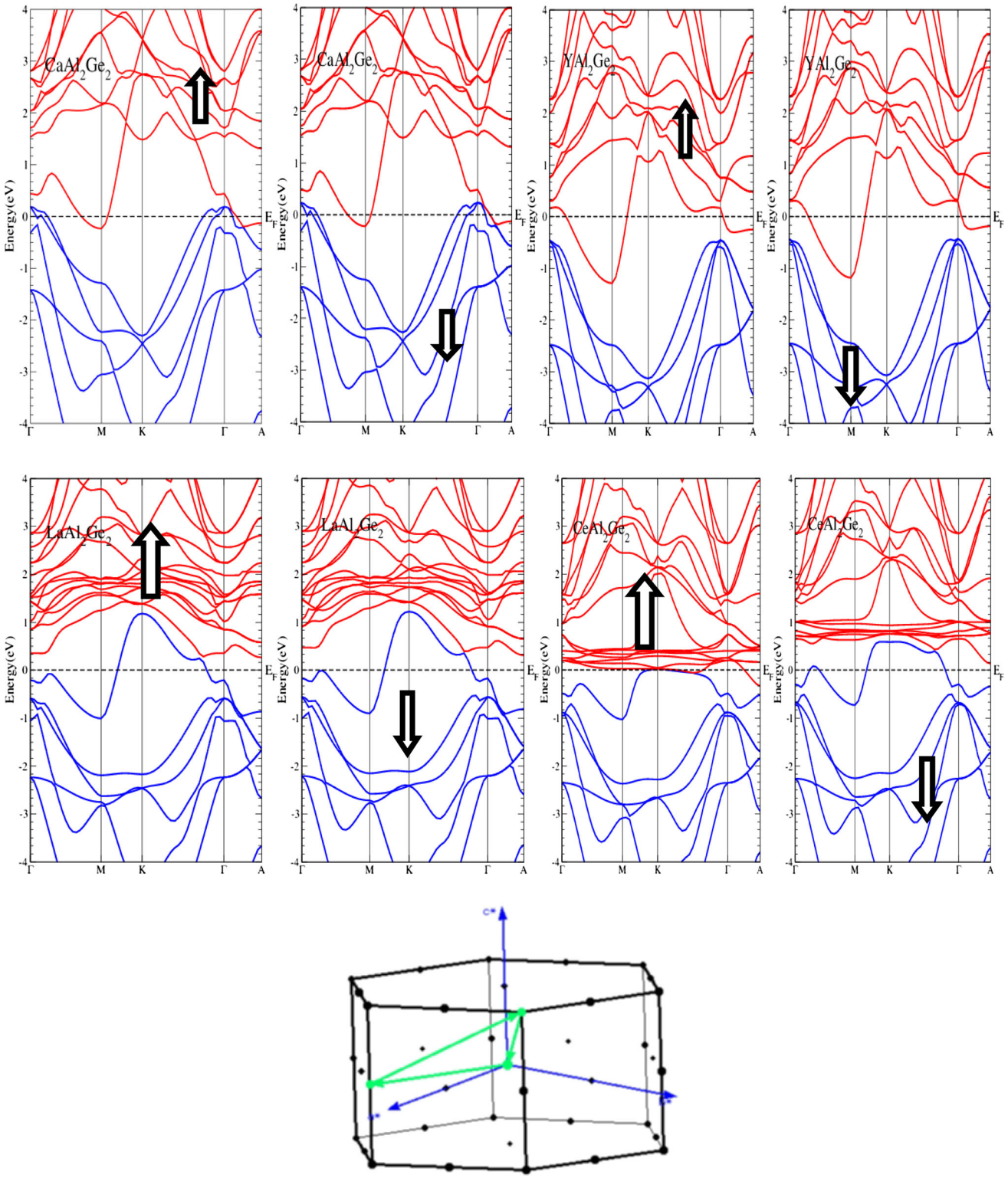

Fig. 3 Band structures of $LmAl_2Ge_2$ compounds in ferromagnetic phase in both directions along with the Brillouin zone

The conduction band (CB) minima illustrate that principal dispersion occurs along with basal plane M directions for $CaAl_2Ge_2$ and YAl_2Ge_2 compounds, respectively, while the compounds $LaAl_2Ge_2$ and $CeAl_2Ge_2$ valance band maxima principal dispersion occurs along with K symmetry point while calculating through GGA-PBE as shown in Fig. 3. Moreover, the CB minima are mostly due to *d* (Ca, Y, La) and Ce *f* characters, whereas the maxima

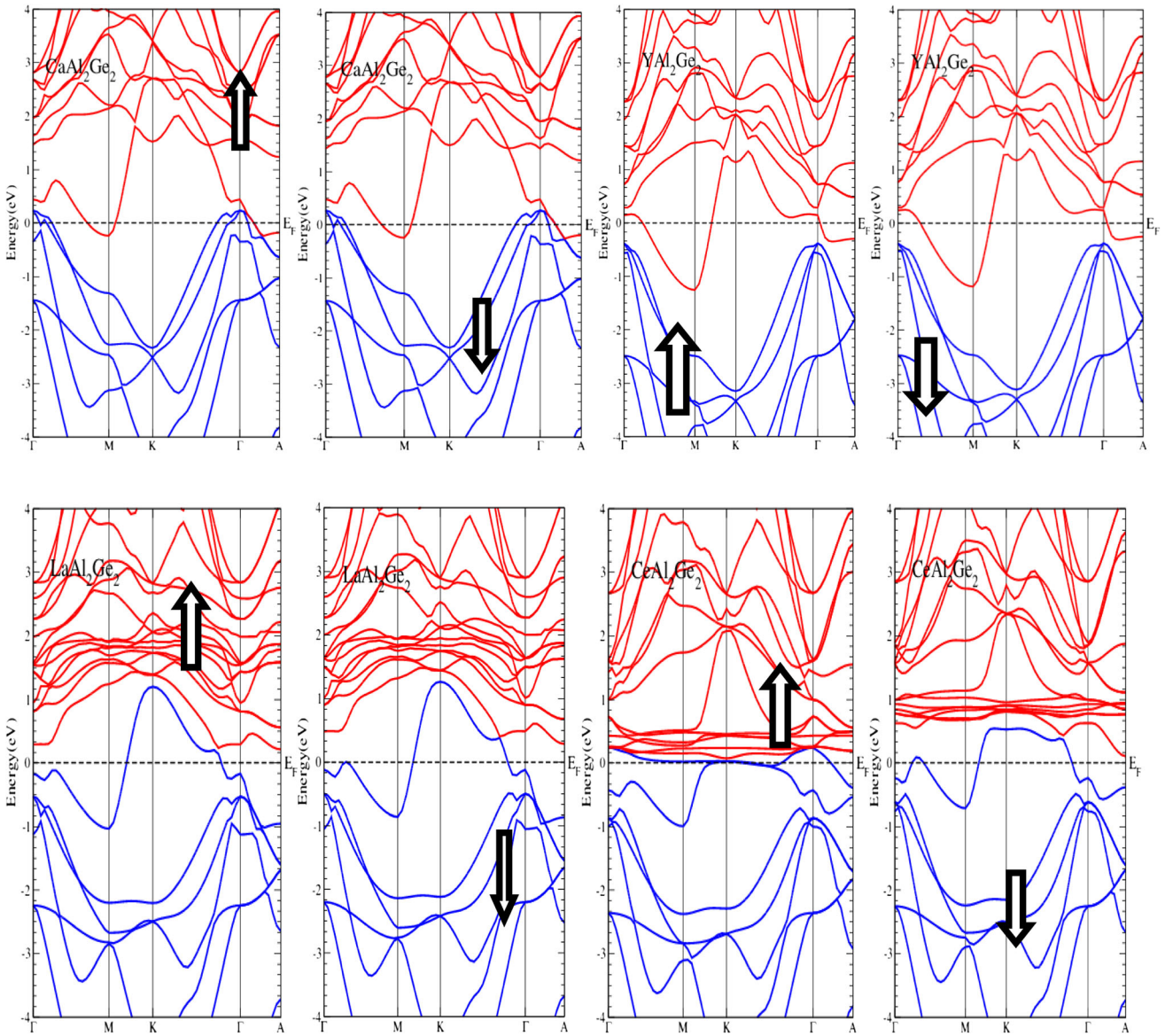

Fig. 4 Band structures of $LmAl_2Ge_2$ compounds in ferromagnetic phase using GGA + U in both directions

of VB are mostly composed of *p* character contributing from the Al/Ge elements in both spin directions. However, there are some differences due to the more continued *d* orbitals appears in $CaAl_2Ge_2$ and YAl_2Ge_2 compounds, the overlap among the *p* (Al, Ge) and the *d* (Ca, Y, La) orbitals twist into stronger side. Consequently, the overlaps are sufficient between the both bands in all compounds.

When the GGA + U potential is applied, a clear split in the bands is seen, but still the compounds depict the metallic nature. In Fig. 4, the minima of conduction band of the $CaAl_2Ge_2$, YAl_2Ge_2 and $LaAl_2Ge_2$ compounds cross the E_f at high symmetry *M* in both spin channels, whereas the $CeAl_2Ge_2$ compound just touches the E_f within spin-up and spin-down valance band crossing the E_f at high symmetry *K* point, which confirm the metallic behavior of these compounds as reported in the previous published work [28].

3.3. Density of states

The projected total and partial density of states for $LmAl_2Ge_2$ compounds is shown in Fig. 5. Moreover, to observe more about the various partial contributions of s, p, d as well as f states of $LmAl_2Ge_2$ compounds, we have plotted total (TDOS) and partial (PDOS) density of states versus energy of $LmAl_2Ge_2$ compounds in the range between − 10 and 10 eV in ferromagnetic phase while computing (GGA + U) approximation potential in both orientations which are examined in Fig. 5.

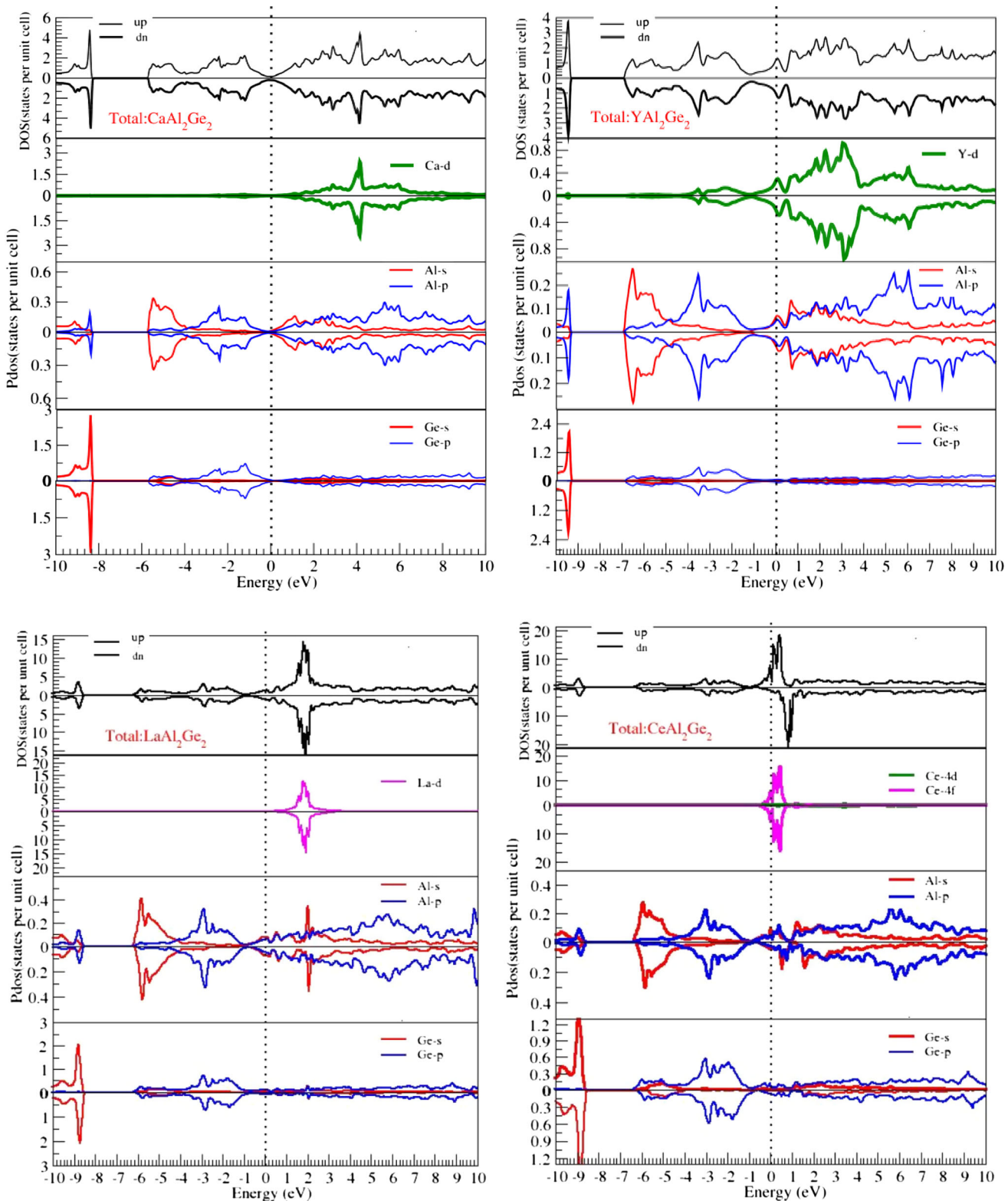

Fig. 5 Designed DOS of $LmAl_2Ge_2$ compounds in ferromagnetic phase using GGA + U in both directions

Though the total projected DOS curves confirm metallic nature for all the under-study compounds because of their partial projected s, p, d and f states traversing the E_f in both spin channels. It clears from the total projected DOS that the foremost contribution at E_F begins from *d* (Ca, Y) whereas La *(d)* and Ce 4*d*/4*f* states. Moreover, there is a

generous hybridization of *d* (Ca, Y) and La*(d)* and Ce 4*d*/4*f* states with *p* (Al, Ge) states present between the conduction/valence band domains of both spin channels.

The foremost contribution in $CaAl_2Ge_2$, YAl_2Ge_2 and $LaAl_2Ge_2$ compounds are due to *d* (Ca, Y, La) state which become visible predominantly in the conduction band-domain whereas minor contribution in valence band-domain of both spin channels and broaden over the entire energy, whereas in the leftover $CeAl_2Ge_2$ compound 4*d* state remained with the appearance of 4*f* state noticeably seen in Ce based compound. Furthermore, the Ce 4*f* state appears sharply in conduction band domain in both up- and down-spin channels, while the same 4*f* state passes the Fermi level toward valence band region in the $CeAl_2Ge_2$ compounds in both up and down channels. Lastly, the slight contribution of *s* and *p* (Al, Ge) states is moderately similar throughout the overall energy range in all studied compounds within the chief leading contribution of *p* (Al, Ge) state along with the negligible contribution of *s (*Al, Ge) states in the conduction and valence domains of both spin directions. The entire states vanished in the energy ranges almost from − 8.5 to − 7 eV which is mainly due to flat band views in the entire band structure of the compounds as noticeably examined in up and down directions. Generally, projected DOS of our reported compounds shows metallic behavior across the E_f in both spin modes.

3.4. Magnetic properties

To gain more enlightening data and wide-ranging perceptive concerning with magnetic properties, we have evaluated the local moments and magnetic interactions in $LmAl_2Ge_2$ compounds through PBE-GGA and so-called GGA + *U* as renowned in Table 2. The positive value of magnetic moment reveals that the magnetic-based state for $LmAl_2Ge_2$ compounds is ferromagnetic. The calculations throughout GGA + *U* gives higher values for $CaAl_2Ge_2$ while lesser for YAl_2Ge_2, $LaAl_2Ge_2$ and $CeAl_2Ge_2$ as compared to GGA-PBE, since it treats to bound (localized d/f-shell) electrons of Ca/(Y, Al, Ce) atoms moreover slightly enhance/reduce its magnetic moment (MM) in contrast within GGA-PBE. The whole cell magnetic moments are primarily composed of (Lm = Ca, Y, La, Ce) atoms along with tiny contributions of interstitial site and Al/Ge. The Lm atom has large magnetic moments from other connected atoms in $LmAl_2Ge_2$ compound. According to magnetic moment investigation, we have remarked that the magnetic moment of (Lm = Ca, Y, La, Ce) atoms is larger with respect to Al/Ge atoms which is essentially because the d/f-state of the (Ca, Y, La, Ce) atoms appears leadingly over the whole energy range in up-spin and down-spin types, as mentioned in the projected DOS calculations. The primary source of magnetization comes from unoccupied *d* (Ca, Y, La) and *f* (Ce) states. Furthermore, the *d* (Ca, Y, La) and (Ce)-f states are demonstrating the partially filled sub-*d as well as d* states. This noticeably initiates weak ferromagnetism in the under-studied compounds. From another point of view, the values of magnetic moment describe the reliable sign of Al/Ge atoms at all sites in the primitive cell on the whole giving rise to small contribution. So, the aluminum and calcium site is antiparallel to the entire MM of $CaAl_2Ge_2$, while Y/La/Ce elements site polarized parallel to their own compounds. In addition to this, the considered values of the MM throughout both schemes at overall cell and interstitial site for $LmAl_2Ge_2$ compound support the net MM, while Al opposes in $CaAl_2Ge_2$ and Ge opposes in YAl_2Ge_2 and $CeAl_2Ge_2$, respectively. The smaller MM values of

Table 2 Magnetic moments of the interstitial region (m^{inte}), single atoms ($M^{Ca/Y/La/Ce}$) and overall cell for $LmAl_2Ge_2$ (Lm = Ca, Y, La, Ce) compounds utilizing both schemes (Bohr magnetrons μ_B)

Compounds	m^{inte}	$M^{Ca/Y/La/Ce}$	m^{Al}	M^{Ge}	m^{cell}
$CaAl_2Ge_2$ (PBE-GGA)	− 0.01923 0.02622	− 0.00055	− 0.00235	0.00289	− 0.01872
GGA + U	–	− 0.01073	− 0.00623	0.01963	0.04228
Exp./other calc		–	–	–	–
YAl_2Ge_2 (PBE-GGA)	0.06856 0.04815	0.02799 0.02461	0.00130 0.00065	− 0.00243	0.09429
GGA + U	–	–	–	− 0.00210	0.06987
Exp./other calc				–	–
$LaAl_2Ge_2$ (PBE-GGA)	0.06066 0.21420	0.01539	0.00117	− 0.00007 0.00646	0.07823
GGA + U	–	0.04121	0.00632	–	0.28098
Exp./other calc		–	–		–
$CeAl_2Ge_2$ (PBE-GGA)	0.54961 0.35940	0.94474 0.95464	0.02436 0.00813	0.00298	1.54903
GGA + U	–	–	–	− 0.00176	1.32678
Exp./other calc				–	–

$CaAl_2Ge_2$, YAl_2Ge_2 and $LaAl_2Ge_2$ confirm that these compounds have week ferromagnetic metallic behavior, while $CeAl_2Ge_2$ compound shows stronger ferromagnetic behavior. The accuracy of GGA + U over GGA is tabulated in Table 2.

4. Conclusions

We have summarized the structural, electronic and magnetic structures of $LmAl_2Ge_2$ basal compounds $CaAl_2Ge_2$, YAl_2Ge_2, $LaAl_2Ge_2$, and $CeAl_2Ge_2$. The spin-polarized configurations were constantly clarified by so-called GGA + U calculations employing U_{eff} = 7 eV. The FM configurations are much stable than the PM configuration. The lattice parameters are in appropriate correspondence with the available experimental values. The electronic properties reveal the metallic nature of these compounds. The magnetic moments indicate that they are weak ferromagnetic compounds.

References

[1] K Masumot and W A McGahan *MRS Bull.* **21** 44 (1996).
[2] L M Schetky *MRS Bull.* **21** 50 (1996)
[3] Z Zada, A Laref, G Murtaza, A Zeb and A Yar *Int. J. Modern Phys. B* **33** 1950199 (2019)
[4] Z Zada *et al*. *Physica B: Condensed Matter* **607** 412866 (2021)
[5] A A Khan, W Khan, A Khan, A Laref, A Zeb and G Murtaza *Mater. Res. Exp.* **6** 066102 (2019)
[6] Z Zada, H Ullah, R Zada, A A Khan, A Mahmood and S M Ramay *Eur. Phys. J. Plus* **136** 371 (2021)
[7] R Bibi *et al*. *J. Solid State Chem.* **302** 122388 (2021)
[8] M I Katsnelson, V Yu Irkhin, L Chioncel, A I Lichtenstein and R A de Groot *Rev. Modern Phys.* **80** 315 (2008)
[9] A Hirohata and K Takanashi *Journal of Physics D: Applied Physics* **47** 193001 (2014)
[10] P Paufler *American Society for Metals. Metals Park. Ohio.* **1** 3258 (1987)
[11] P Klüfers and A Mewis *Zeitschrift für Naturforschung B* **32** 753 (1977).
[12] P Klüfers and A Mewis *Zeitschrift für Kristallographie-Crystalline Materials* **169** 135 (1984)
[13] A Artmann, A Mewis, M Roepke and G Michels *Zeitschrift für anorganische und allgemeine Chemie* **622** 679 (1996)
[14] U H Schuster and O H Fischer *Zeitschrift für Naturforschung B* **34** 1169 (1979).
[15] O H Fischer and U H Schuster *Zeitschrift für Naturforschung B* **35** 1322 (1980).
[16] G Zwiener, H Neumann and U H Schuster *Zeitschrift für Naturforschung B* **36** 1195 (1981)
[17] I Grund, U H Schuster and P Müller *Zeitschrift für anorganische und allgemeine Chemie* **515** 151 (1984)
[18] V V Nemoshkalenko et al *Ukrainskij Fizicheskij Zhurnal* **26** 1831 (1981)
[19] V V Nemoshkalenko and N V Antonov *Kiev Izdatel Naukova Dumka* (1985)
[20] S O Zarechnyuk *Akad. Nauk Ukr. RSR. Ser. A* **32** 753 (1970)
[21] R Xesper and G H von Schnering *Zeitschrift für Naturforschung B* **37** 1514 (1982)
[22] H Flandorfer and P Rogl *J. Solid State Chem.* **127** 308 (1996).
[23] A A Murav'eva, S O Zarechnyuk and Gladyshevskii, E. I. Inorg. Mat. **7** 34 (1971)
[24] C Kranenberg, D Johrendt and A Mewis *Zeitschrift für anorganische und Allgemeine Chemie* **625** 1787 (1999)
[25] C Kranenberg et al *Solid State Sci.* **2** 215 (2000).
[26] K Rajput and S Vitta *J. Mater. Sci. Mater. Electron.* **27** 10303 (2016).
[27] S Bobev et al *J. Solid State Chem.* **178** 2091 (2005).
[28] C Kranenberg, D Johrendt and A Mewis *Solid State Sci.* **4** 261 (2002)
[29] J E Gladishevskij, I P Kripjakevic and I O Bodak *Ukr. Fiz. Zh. (Russ. Ed.)* **12** 447 (1967)
[30] Q G Huang and D R Miao *Phys. B Condens. Matter* **391** 174 (2007).
[31] B Fadila et al *J. Mag. Mag. Mater.* **448** 208 (2018).
[32] A Mentefa et al *J. Supercond. Novel Mag.* **34** 269 (2021).
[33] A Moussali, B M Amina, B Fassi, I Ameri, M Ameri and Y Al-Douri *Indian J. Phys.* **94** 1733 (2020)
[34] M Ayad et al *Indian J. Phys.* **94** 767 (2020).
[35] K Bidai et al *Arch. Metallur. Mater.* **62** 865 (2017).
[36] A A Khan, A U Rehman, A Laref, M Yousaf and G Murtaza *Zeitschrift für Naturforschung A* **73** 965 (2018)
[37] N Guechi, A Bouhemadou, Y Medkour, Y Al-Douri, R Khenata and S Bin-Omran *Philos. Mag.* **100** 3023 (2020)
[38] G Murtaza et al *Eur. Phys. J. Plus* **136** 173 (2021).
[39] A Bekhti-Siad et al *Chin. J. Phys.* **56** 870 (2018).
[40] A A Khan, M Yaseen, A Laref, and G Murtaza *Phys. B Condens. Matter* **541** 24 (2018)
[41] P Hohenberg and W Kohn *Phys. Rev.* **136** B864 (1964).
[42] W Kohn and L J Sham *Phys. Rev.* **140** A1133 (1965).
[43] P Blaha, K Schwarz, G K Madsen, D Kvasnicka and J Luitz **60** (2001)
[44] J P Perdew, K Burke and M Ernzerhof *Phys. Rev. Lett.* **77** 3865 (1996)
[45] A I Liechtenstein, V I Anisimov and J Zaanen *Physical Review B* **52** R5467 (1995)
[46] O Bengone, M Alouani, P Blöchl and J Hugel Physical Review B **62** 16392 (2000)
[47] H J Monkhorst and J D Pack *Phys. Rev. B* **13** 5188 (1976).
[48] J D Pack and H J Monkhorst *Phys. Rev. B* **16** 1748 (1977).
[49] Q D Gibson *et al*. *Phys. Rev. B* **91** 085128 (2015)
[50] H Flandorfer et al *J. Solid State Chem.* **137** 191 (1998).
[51] M Ameri, F Bennar, S Amel and I Ameri *Y Al-Douri and D Varshney Phase Transitions* **89** 1236 (2016).
[52] M Ameri *et al*. *Chin. J. Phys.* **53** 040802 (2015)
[53] S Touam et al *Bulletin of Materials Science* **43** 1 (2020).
[54] M Ameri et al *Materials science in semiconductor processing* **27** 368 (2014).
[55] Y Al-Douri, M Ameri, A Bouhemadou, and K M Batoo *Physica Status Solidi (B)* **256** 1900131 (2019)
[56] K Boudiaf, A Bouhemadou, Y Al-Douri, R Khenata, S Bin-Omran, and N Guechi *J. Alloys Compd.* **759** 32 (2018)
[57] M Cococcioni and S De Gironcoli *Phys. Rev. B* **71** 035105 (2005)
[58] A Otero-de-la-Roza, D Abbasi-Pérez and V Luaña *Comput. Phys. Commun.* **182** 2232 (2011)